

## Experimental Demonstration of Violations of the Second Law of Thermodynamics for Small Systems and Short Time Scales

G. M. Wang,<sup>1</sup> E. M. Sevick,<sup>1</sup> Emil Mittag,<sup>1</sup> Debra J. Searles,<sup>2</sup> and Denis J. Evans<sup>1</sup>

<sup>1</sup>Research School of Chemistry, The Australian National University, Canberra ACT0200, Australia

<sup>2</sup>School of Science, Griffith University, Brisbane QLD4111, Australia

(Received 4 March 2002; published 15 July 2002)

We experimentally demonstrate the fluctuation theorem, which predicts appreciable and measurable violations of the second law of thermodynamics for small systems over short time scales, by following the trajectory of a colloidal particle captured in an optical trap that is translated relative to surrounding water molecules. From each particle trajectory, we calculate the entropy production/consumption over the duration of the trajectory and determine the fraction of second law-defying trajectories. Our results show entropy consumption can occur over colloidal length and time scales.

DOI: 10.1103/PhysRevLett.89.050601

PACS numbers: 05.70.Ln, 05.40.-a

Inventors and engineers endeavor to scale down machines and engines to nanometer sizes for a wide range of technological purposes. However, there is a fundamental limitation to miniaturization as small engines are *not* simple rescaled versions of their larger counterparts. If the work performed during the duty cycle of any machine is comparable to thermal energy per degree of freedom, then one can expect that the machine will operate in “reverse” over short time scales. That is, heat energy from the surroundings will be converted into useful work allowing the engine to run backwards. For larger engines, we would describe this as a violation of the second law of thermodynamics, as entropy is consumed rather than generated. This has received little attention in the nanotechnology literature, as there was no quantitative description of the probability of entropy consumption in such small engines. The only thermodynamic statement available was the second law itself, stating that, for large systems and over long times, the entropy production rate is necessarily positive. Even the foundations of statistical mechanics were unsettled as thermodynamicists questioned how the second law of thermodynamics could be reconciled with reversible microscopic equations of motion. Loschmidt’s paradox states that in a time reversible system, for every phase-space trajectory there exists a time-reversed antitrajectory [1]. As the entropy production of a trajectory and its conjugate antitrajectory are of identical magnitude but opposite sign, then, so the argument goes, one cannot prove that entropy production is positive.

However, in 1993, a resolution and quantitative description of violations of the second law in finite systems was given by the fluctuation theorem (FT) of Evans *et al.* [2]. The theorem provides an analytic expression for the probability that the dissipative flux flows in the direction reverse to that required by the second law of thermodynamics. In other words, the theorem predicts appreciable and measurable violations of the second law for small systems over short time scales. Specifically, the theorem relates the probability,  $\text{Pr}$ , of observing a phase-space

trajectory of duration  $t$  with entropy production  $\Sigma_t = A$ , to that of a trajectory with the same magnitude of entropy change, but where the entropy is consumed or absorbed:

$$\frac{\text{Pr}(\Sigma_t = A)}{\text{Pr}(\Sigma_t = -A)} = \exp(A). \quad (1)$$

As the entropy production,  $\Sigma_t$ , is an extensive property, its magnitude scales with system size and observation time or trajectory duration  $t$ . Thus, the FT also shows that as the system size gets larger or the trajectory duration becomes longer, entropy-consuming trajectories become unlikely, and we recover the expected second law behavior. Much of the work done in developing and extending the theorem was accomplished by theoreticians [3–6] and mathematicians [7,8] interested in nonequilibrium statistical mechanics [9–11]. A few demonstrations of the theorem have been provided with computer simulations [3,12–14]. However, there has been no practical experimental demonstration of the predictions of the theorem. A pedagogical review of the FT was published recently [15].

In this Letter, we demonstrate and quantitatively confirm the predictions of the FT for transient systems [3] by experimentally following the trajectory of a colloidal particle in an optical trap. An optical trap is formed when the micron-sized transparent particle whose index of refraction is greater than the surrounding medium, is located within a focused laser beam. The refracted rays differ in intensity over the volume of the sphere and exert a pico-Newton scale force ( $\text{pN} = 10^{-12}\text{N}$ ) on the particle, drawing it towards the region of highest light intensity [16]. The optical trap is harmonic near the focal point: the force acting on a colloidal particle positioned at  $\mathbf{x}$  within a trap centered at  $\mathbf{x}_0$  is  $\mathbf{F}_{\text{opt}} = -k(\mathbf{x} - \mathbf{x}_0)$ , where  $k$  is the trapping constant which can be tuned by adjusting the laser power. In our experiment, the optical trap translates relative to the solvent at a velocity  $\mathbf{v}_{\text{opt}}$ , starting from time  $t = 0$ . From the particle’s temporal position,  $\mathbf{x}(t)$ , and the optical forces acting on the particle during the trajectory,

we can calculate  $\Sigma_t$ , the entropy production along a trajectory of duration  $t$ . The particle's dimensionless entropy production, integrated over the duration of the trajectory [12] is

$$\Sigma_t = (k_B T)^{-1} \int_0^t ds \mathbf{v}_{\text{opt}} \cdot \mathbf{F}_{\text{opt}}(s), \quad (2)$$

where  $T$  is the temperature of the heat sink surrounding the system [17]. We show that the occurrence of antitrajectories, or trajectories for which entropy is consumed ( $\Sigma_t < 0$ ) quantitatively follows the prediction of an integrated form of the FT, expressed for transient systems [18]. Moreover, our experiment provides the first evidence that the appreciable and measurable violations of the second law of thermodynamics in small systems occur not only at simulation time scales (femtoseconds), but also at colloidal time and length scales (seconds).

The experimental setup consists of a Nikon DIAPHOT 300 inverted microscope equipped with a 100 $\times$  (NA = 1.3) oil immersion objective lens, an infrared laser ( $\lambda = 980$  nm, 1 W) for trapping micron-sized particles, a servo-motor controlled microscope stage with fine piezo-controlled translation in the  $x - y$  plane, and a quadrant photodiode sensor for detection of particle position. Laser power, objective focus, and servo-motor controlled motion of the microscope stage are controlled by a dedicated computer through interfaces developed by Cell Robotics Inc. USA. A 1.0 ml glass sample cell containing roughly 100 6.3  $\mu\text{m}$  diameter latex particles (Interfacial Dynamics Co.) in water is mounted on the microscope stage. Initially, a latex particle is trapped under full laser power, which is then reduced to 1%. The trap center or focal point is  $\sim 50$   $\mu\text{m}$  from the bottom of the sample cell. An image of the trapped latex particle is projected onto a 3 mm  $\times$  3 mm quadrant photodiode which detects the position of the particle to 15 nm. Our circuitry has a bandwidth of about 500 Hz. We set our sampling rate at 1 kHz to ensure an adequate amount of data without appreciable signal distortion. The optical trapping force is calibrated from the bead's drag coefficient, calculated using Stokes equation. The Stokes drag coefficient is consistent with the experimentally determined diffusion coefficient of the latex bead.

The particle trajectories are monitored within weak optical traps using very small translations of the stage relative to the fixed trap, in order that the duration of the transient period is maximized. For all trajectories, the trapping force is generated with only 1% laser power which corresponds to a trapping constant of  $k \sim 0.1$  pN/ $\mu\text{m}$ , or  $1 \times 10^{-5}$  pN/ $\text{\AA}$ . Thus, from the particle position, we can resolve forces on the order of 2 femto-Newtons (0.002 pN). For each trajectory, we first record the particle position in the absence of any stage translation for a minimum of 2 sec to record average values of  $\mathbf{x}_0$ , and then initiate stage translation at  $t = 0$ , maintaining the

1 kHz recording of particle position. The stage is translated at a constant velocity  $-\mathbf{v}_{\text{opt}} = 1.25$   $\mu\text{m/s}$  by feeding an 80 V 0.01 Hz triangular wave signal to the stage-mounted piezocrystals and stage motion and particle position are recorded for up to 10 sec, when the particle attains its averaged, steady-state velocity. Over 500 transient trajectories are recorded using this automated procedure.

Figure 1 shows the distribution of time-averaged entropy production,  $\Sigma_t/t$ , in 540 particle trajectories at times up to 2 sec after the start of stage translation. The entropy production is calculated by summing the scalar product of particle displacement and stage velocity according to Eq. (2), for successive intervals of  $\Delta t = 10^{-3}$  sec up to  $t$ . For  $t = 10^{-2}$  sec, the trajectories are distributed nearly symmetrically about  $\Sigma_t = 0$  with entropy-consuming and entropy-producing trajectories of nearly equal numbers. At longer times, the entropy-consuming trajectories ( $\Sigma_t < 0$ ) occur less often and the mean entropy production of the trajectories shifts towards more positive numbers, in accord with the FT. At longer times, that is, for  $t$  greater than a few seconds, these entropy-consuming trajectories cannot be observed, as predicted from the second law of thermodynamics.

As the number of trajectories collected and analyzed is small, it is easier to examine an integrated form of the FT [13]. This integrated form, or the IFT, describes the probability of observing entropy-consuming trajectories to that of entropy-producing trajectories, and is given by

$$\frac{\Pr(\Sigma_t < 0)}{\Pr(\Sigma_t > 0)} = \langle \exp(-\Sigma_t) \rangle_{\Sigma_t > 0}, \quad (3)$$

where the brackets denote an average over all entropy-producing trajectories. Experimentally, we determine the left-hand side of the IFT by counting the number of entropy-consuming ( $\Sigma_t < 0$ ) and entropy-producing

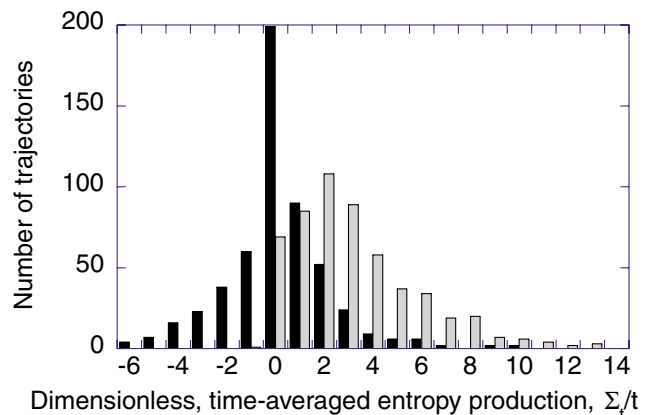


FIG. 1 (color online). Histogram of the dimensionless, time-averaged entropy production,  $\Sigma_t/t$ , from 540 experimental trajectories of a colloidal particle in an optical trap at times  $t = 10^{-2}$  (black bars) and  $t = 2.0$  (gray bars) seconds after initiation of stage translation. The bin size is  $\Delta \Sigma_t/t = 1.0$ .

( $\Sigma_t > 0$ ) trajectories of duration  $t$ . The right-hand side is determined by averaging the negative exponential of the dimensionless entropy production over the subset of entropy-producing trajectories of time  $t$ . Figure 2 plots the experimentally determined left- and right-hand sides of the IFT as a function of the time along the trajectories. In accord with the theorem these experimental quantities are, to within statistical error, equivalent for trajectories of up to 3 sec. The detector resolves distances down to 15 nm and, consequently, this limits our ability to discriminate between small positive and small negative values of  $\Sigma_t$  whose magnitude is less than  $3.0 \times 10^{-4}$ . This discrimination error is minimal, but may contribute to the anomalous number ratio in the initial 0.02 to 0.03 sec of Fig. 2. There are other possible sources of this small error, including unavoidable, but minimal, transients associated with initiation of the stage translation.

It is instructive to compare these experimental results with computer simulation. We have constructed a molecular dynamics (MD) simulation which mimics the optical tweezers experiment and allows us to track the trajectory of a single particle which “feels” the optical trap in a solution of interacting particles which are unaffected by the trap, but are otherwise identical. The optical trap is initially stationary, but moves with constant velocity during a “simulated trajectory” from  $t = 0$  to  $t_{\max}$ . In addition, we include a subset of identical particles which are confined to two layers which form a wall along one dimension and are restricted from moving out of the wall via a restoring force (see inset of Fig. 3). These wall particles act as a momentum and heat sink/source. There are  $N = N_s + N_w$  particles in the simulation, where  $N_s$  is the number of solution particles, of which the first is the optically trapped particle, and  $N_w$  is the number of wall particles. The coordinates and momenta of the  $N$  particles

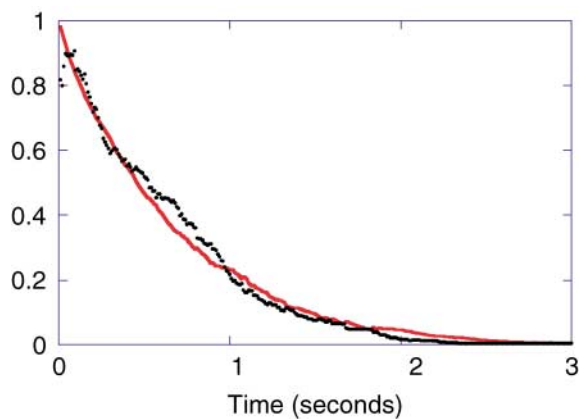


FIG. 2 (color online). The number ratio of entropy-consuming ( $\Sigma_t < 0$ ) to entropy-producing ( $\Sigma_t > 0$ ) trajectories (data points) and the entropy production averaged over entropy-producing trajectories,  $\langle \exp(-\Sigma_t) \rangle_{\Sigma_t > 0}$  (line) versus duration,  $t$ , of 540 experimental trajectories. In accord with the IFT, both experimentally determined measures agree over time.

( $\mathbf{q}_1, \mathbf{q}_2, \dots, \mathbf{q}_N, \mathbf{p}_1, \dots, \mathbf{p}_N$ ) are given by the equations of motion

$$\dot{\mathbf{q}}_i = \frac{\mathbf{p}_i}{m} \quad \text{for } 1 \leq i < N, \quad (4)$$

$$\dot{\mathbf{p}}_i = \sum_{j \neq i}^N \mathbf{F}_{ij} + \delta_{1i} \mathbf{F}_{\text{opt}} \quad \text{for } 1 \leq i \leq N_s, \quad (5)$$

$$\dot{\mathbf{p}}_i = \sum_{j \neq i}^N \mathbf{F}_{ij} + \mathbf{F}_i^w - \alpha \mathbf{p}_i \quad \text{for } (N_s + 1) \leq i \leq N_w. \quad (6)$$

The interaction force acting between any pair of particles,  $i$  and  $j$ , separated a distance  $q$  is  $\mathbf{F}_{ij} = -d\phi(q)/d\mathbf{q}$  where the pair potential is  $\phi(q) = 4(q^{-12} - q^{-6})$  for interparticle distances less than a cutoff of  $2^{1/6}$  and  $\phi(q) = 0$  otherwise. Acting only on the first particle is an optical force,  $\mathbf{F}_{\text{opt}} = -k[\mathbf{q}_1 - \mathbf{q}_0(t)]$ , where  $k$  is the optical trapping constant and the position of the trap center is  $\mathbf{q}_0(t) = \mathbf{q}_0(0) + \mathbf{v}_{\text{opt}}t$  during the simulated trajectory  $0 < t < t_{\max}$  and is stationary at  $\mathbf{q}_0(0)$  otherwise. For the wall particles,  $\mathbf{F}_i^w = -k^w(\mathbf{q}_i - \mathbf{q}_i^{\text{xtal}})$  is a force acting to restore wall particles to their initial crystalline configuration at  $\mathbf{q}_i^{\text{xtal}}$  and  $\alpha$  is the Nosé-Hoover thermostat multiplier [19]. A time step of  $\delta = 0.001$  is used and the maximum duration of a simulated trajectory is  $t_{\max} = 5000\delta$ . The system is allowed to equilibrate for  $10^4$  time steps during which the optical trap is stationary at  $\mathbf{q}_0(0)$ . After each simulated trajectory, we return the momenta and coordinates of the particles to their initial values and allow the system to evolve for a further

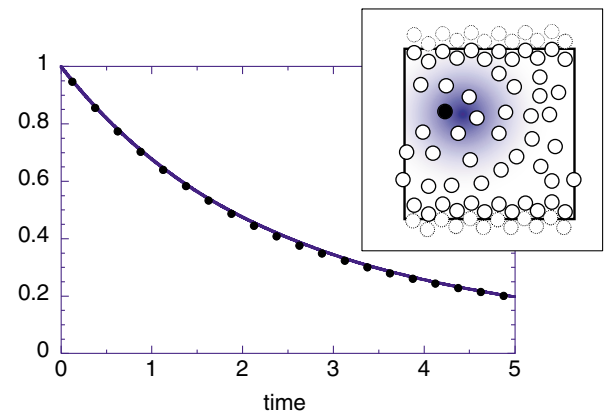


FIG. 3 (color online). The number ratio of entropy-consuming ( $\Sigma_t < 0$ ) to entropy-producing ( $\Sigma_t > 0$ ) trajectories (data points) and the entropy production averaged over entropy-producing trajectories,  $\langle \exp(-\Sigma_t) \rangle_{\Sigma_t > 0}$  (line) versus duration,  $t$ , calculated from 343 500 simulated trajectories. The inset depicts the 2D MD simulation cell (to scale) containing  $N_s = 32$  particles at a number density of 0.30,  $N_w = 24$  wall particles, and an optical trap with constant  $k = 1$  that translates at  $v_{\text{opt}} = 0.5$ . Only the first particle, depicted by the filled circle, “feels” the optical trap, represented by the shaded region. The initial temperature of both wall and solution particles was  $T = 1.0$ . All MD quantities are reported in reduced units.

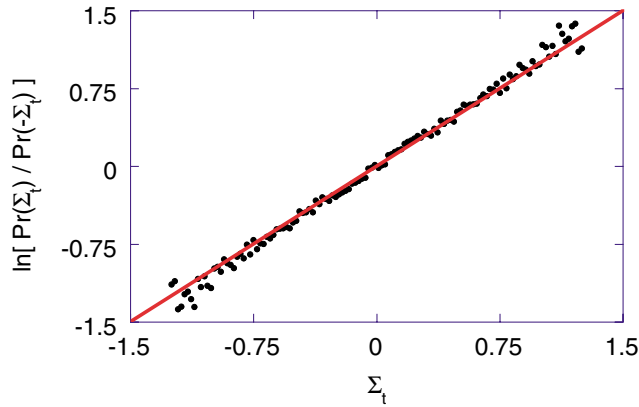


FIG. 4 (color online). Logarithm of the number ratio of trajectories with entropy production  $-\Sigma_t$  to those with entropy production  $\Sigma_t$  versus  $\Sigma_t$ , found from over 310 000 MD trajectories.

200 time steps with a stationary trap. It is important to emphasize that we do not construct conjugate trajectory/antitrajectory pairs, but rather we sample the deterministic trajectories which start from a canonical ensemble of equilibrium starting momenta and coordinates and measure the probability of occurrence of antitrajectories over time.

Figure 3 shows the left- and right-hand sides of the IFT, Eq. (3), as a function of the duration of the simulated trajectories. Each point corresponds to the number ratio of entropy-consuming to entropy-producing trajectories. As in Fig. 2, the line represents the average of the exponential of the entropy production over the subset of simulated trajectories over which entropy is generated. Both simulated and experimental trajectories show the exponential decrease in the number of entropy-consuming trajectories with time. The advantage of simulation over experiment is that many more trajectories can be analyzed and it is then possible to investigate not only the IFT but the FT itself, Eq. (1). Figure 4 shows the ratio of the probabilities of finding a trajectory of entropy production  $\Sigma_t = A$  to that of finding a trajectory of same magnitude of entropy change, but where the entropy is consumed or adsorbed, as a function of  $A$ . The data fall on the line, which represents the prediction of the FT.

That entropy-consuming trajectories can be discerned for micron-sized particles over time scales on the order of seconds is particularly important to applications of nanomachines and to the understanding of protein motors. The fluctuation theorem points out that as these thermodynamic engines are made smaller and as the time of operation is made shorter, these engines are not simple scaled-down versions of their larger counterparts. As they become smaller, the probability that they will run thermodynamically

in reverse inescapably becomes greater. Consequently, these results imply that the fluctuation theorem has important ramifications for nanotechnology and indeed for how life itself functions.

D.J.S. acknowledges financial support from the Australian Research Council. G. M. W. and E. M. S. thank Dr. Liam Waldron, Facilities Engineer of RSC, for his design and construction of the quadrant photodiode.

- 
- [1] J. Loschmidt, *J. Sitzungsber. der kais. Akad. d. W. Math. Naturw. II* **73**, 128 (1876).
  - [2] D. J. Evans, E. G. D. Cohen, and G. P. Morriss, *Phys. Rev. Lett.* **71**, 2401 (1993).
  - [3] D. J. Evans and D. J. Searles, *Phys. Rev. E* **50**, 1645 (1994).
  - [4] G. E. Crooks, *Phys. Rev. E* **60**, 2721 (1999).
  - [5] G. E. Crooks, *Phys. Rev. E* **61**, 2361 (2000).
  - [6] C. Jarzynski, *Phys. Rev. Lett.* **78**, 2690 (1997).
  - [7] G. Gallavotti and E. G. D. Cohen, *Phys. Rev. Lett.* **74**, 2694 (1995).
  - [8] S. Lepri, L. Rondoni, and G. Benettin, *J. Stat. Phys.* **99**, 857 (2000).
  - [9] P. Gaspard, *Chaos, Scattering, and Statistical Mechanics* (Cambridge University Press, Cambridge, United Kingdom, 1998).
  - [10] J. R. Dorfman, *An Introduction to Chaos in Non-equilibrium Statistical Mechanics* (Cambridge University Press, Cambridge, United Kingdom, 1999).
  - [11] D. Ruelle, *J. Stat. Phys.* **95**, 393 (1999).
  - [12] D. J. Searles and D. J. Evans, *J. Chem. Phys.* **113**, 3503 (2000).
  - [13] G. Ayton, D. J. Evans, and D. J. Searles, *J. Chem. Phys.* **115**, 2033 (2001).
  - [14] D. J. Evans, D. J. Searles, and E. Mittag, *Phys. Rev. E* **65**, 051105 (2001).
  - [15] D. J. Evans and D. J. Searles, *Adv. Phys.* (to be published).
  - [16] A. Ashkin, *Proc. Natl. Acad. Sci. U.S.A.* **94**, 4853 (1997).
  - [17] E. Mittag, D. J. Searles, and D. J. Evans, *J. Chem. Phys.* **116**, 6875 (2002).
  - [18] In the original derivations of the FT [2,7], the trajectories were stipulated to be at “steady-state” with  $t$  large and representing a time interval, anywhere within the steady-state trajectory, over which the entropy production is averaged. In the experiment described herein, the FT is applied to transient trajectories, where an external field (which translates the trap) is applied starting at  $t = 0$ . The FT, Eq. (1), is unchanged except that  $t$  now denotes the time interval starting from the initiation of the external field, as well as the time over which the entropy production is averaged. Expressed in this way, the FT has been referred to in the literature as the TFT or transient fluctuation theorem [3,12,15].
  - [19] D. J. Evans and G. P. Morriss, *Statistical Mechanics of Non Equilibrium Liquids* (Academic Press, London, 1990).